

Development and Validation of a Nomogram Integrating Body Composition and Inflammatory Markers to Predict Concurrent Chemoradiotherapy Response in Locally Advanced Cervical Cancer

Lina Liu¹, Qianqian Zhang¹, Lele Liu¹, Zhenzhen Wu¹, Xingxia Zhang², Jianli Qiao³, Mali Chen¹

¹Department of Obstetrics and Gynecology, Gansu Provincial Maternal and Child Health Hospital (Gansu Provincial Central Hospital), Lanzhou, Gansu, People's Republic of China; ²Department of Anesthesia, The Third People's Hospital of Gansu Provincial, Lanzhou, Gansu, People's Republic of China; ³Department of General Surgery, The Third People's Hospital of Gansu Provincial, Lanzhou, Gansu, People's Republic of China

Correspondence: Mali Chen, Department of Obstetrics and Gynecology, Gansu Provincial Maternal and Child Health Hospital (Gansu Provincial Central Hospital), Lanzhou, Gansu, People's Republic of China, Email habe.13_mary@126.com

Purpose: To develop and validate a nomogram integrating body composition and systemic inflammatory markers for predicting sensitivity to concurrent chemoradiotherapy (CCRT) in patients with locally advanced cervical cancer (LACC).

Patients and Methods: This single-center retrospective study included 215 patients with FIGO 2018 stage IIB-IVA LACC who received first-line CCRT between September 2020 and September 2024. Patients were randomly assigned to a training set (n=150) and a test set (n=65). Treatment response was assessed approximately 8 weeks after radiotherapy according to RECIST version 1.1. Patients with complete or partial response were classified as CCRT-sensitive, whereas those with stable or progressive disease were classified as CCRT-resistant. Multivariable logistic regression was used to identify independent predictors and construct a nomogram. Model performance was evaluated using receiver operating characteristic (ROC) curves, calibration curves, and decision curve analysis (DCA), and was compared with clinical-only, systemic inflammatory, and body composition models.

Results: Tumor size, platelet-to-lymphocyte ratio, prognostic nutritional index, skeletal muscle index, and visceral adipose index were identified as independent predictors of CCRT sensitivity and were incorporated into the nomogram. The model showed good discrimination, with an area under the ROC curve of 0.796 (95% CI, 0.714–0.878) in the training set and 0.751 (95% CI, 0.618–0.884) in the test set. At the optimal cutoff probability of 0.66, sensitivity and specificity were 75.7% and 72.1% in the training set, and 79.1% and 59.1% in the test set, respectively. Calibration curves showed good agreement, and DCA indicated favorable clinical utility. The nomogram outperformed the three single-domain models.

Conclusion: We developed and internally validated a non-invasive nomogram integrating tumor size, systemic inflammatory markers, and CT-based body composition parameters to predict CCRT sensitivity in LACC. This model may assist in early risk stratification and individualized treatment planning, although external validation in larger multicenter cohorts is still needed.

Keywords: nomogram, concurrent chemoradiotherapy, locally advanced cervical cancer, body composition, inflammatory

Introduction

Cervical cancer continues to impose a substantial global health burden, ranking as the fourth most prevalent cancer and the fourth leading cause of cancer-related mortality among women worldwide.^{1,2} A significant proportion of cervical cancer patients are diagnosed at a locally advanced stage (LACC), classified as stage IIB to IVA according to the International Federation of Gynecology and Obstetrics (FIGO) 2018 staging system.³ For patients with LACC, concurrent chemoradiotherapy (CCRT) is the standard treatment modality, endorsed by international guidelines such as those from the National Comprehensive Cancer Network (NCCN).⁴ Clinical trials have demonstrated that CCRT can reduce the risk of death by 30–35% compared to radiotherapy alone, achieving five-year overall survival (OS) rates of



approximately 70%.^{5–9} Despite these advancements, some patients fail to achieve remission following treatment, and this subgroup is associated with a particularly poor prognosis, with a five-year survival rate of less than 20%.¹⁰ Meanwhile, CCRT itself can lead to complications such as myelosuppression and radiation enteritis, which, in the context of treatment resistance, further limits subsequent therapeutic options and worsens patient outcomes.¹¹ Thus, there is an urgent need for early identification of patients who are unlikely to respond to CCRT.

Traditional prognostic factors for LACC, including tumor stage, histologic type, tumor burden, lymph node status, and performance status, provide only limited precision for individualized response prediction.^{12,13} In recent years, several predictive or prognostic models have been proposed for cervical cancer treated with CCRT. However, most existing models have primarily focused on long-term survival outcomes, such as progression-free survival (PFS) or overall survival (OS), rather than early treatment sensitivity. In addition, many of these models are based mainly on clinico-pathological variables or single-domain biomarkers, which may not fully capture host-related biological heterogeneity relevant to treatment response. At the same time, biomarker-oriented studies suggest that pretreatment host status may provide additional information beyond conventional clinicopathological factors. A tissue-based molecular signature combining ANXA2, NDRG1, and STAT1 has been reported to predict chemoradiotherapy response in cervical cancer, supporting the feasibility of response prediction but also indicating the practical limitations of models that depend on tumor sampling and specialized assays.¹⁴

Emerging evidence suggests that systemic inflammatory markers and CT-derived body composition parameters provide complementary information on the biological and physiological status of cancer patients.^{15–20} Systemic inflammatory biomarkers, such as the neutrophil-to-lymphocyte ratio (NLR), lymphocyte-to-monocyte ratio (LMR), and systemic immune-inflammation index (SII), reflect the interplay between tumor progression, immune status, and nutritional reserve.^{17–20} Likewise, CT-based body composition measures, including skeletal muscle and adipose tissue metrics, offer a non-invasive assessment of metabolic and nutritional condition beyond conventional body mass index.^{16,21} Guo et al²² reported that the combined prognostic value of body composition indicators and systemic inflammatory markers was reliable for survival prediction in patients with LACC after chemoradiotherapy. More recently, He et al²³ developed dual nomograms using the lactate dehydrogenase-to-albumin ratio and clinicopathological indicators to predict short-term therapeutic response and OS in LACC treated with CCRT. Nevertheless, an integrated, readily applicable, non-invasive model specifically designed to predict early CCRT sensitivity by combining routine CT-based body composition parameters with systemic inflammatory and nutritional markers has not been well established.

Therefore, in this single-center retrospective study, we aimed to develop and internally validate a clinically accessible nomogram integrating CT-based body composition parameters and systemic inflammatory markers for predicting early sensitivity to concurrent chemoradiotherapy in patients with LACC. By combining routinely available clinical, laboratory, and imaging-derived variables, we sought to address the limitations of existing single-domain prediction approaches and to provide a more comprehensive tool for predicting early CCRT sensitivity, as defined by RECIST 1.1 criteria. We also compared its performance with clinical-only, inflammatory-only, and body-composition-only models to determine the incremental value of this multidimensional approach.

Methods

Patients

This retrospective study included patients diagnosed with cervical cancer who were admitted to our hospital from September 2020 to September 2024 at the Gansu Provincial Maternal and Child Health Hospital. The inclusion criteria were as follows: (1) histologically confirmed cervical cancer; (2) FIGO stage IIB to IVA according to the 2018 staging system; (3) baseline Karnofsky Performance Status (KPS) score of ≥ 70 ; (4) undergoing first-time treatment; (5) Pre-treatment imaging, including contrast-enhanced pelvic MRI and contrast-enhanced CT of the chest/abdomen/pelvis, with PET-CT performed when CT/MRI findings were equivocal, confirmed the absence of distant metastasis, and (6) availability of complete clinical and pathological data. Exclusion criteria comprised: (1) prior receipt of chemoradiotherapy; (2) contraindications to chemoradiotherapy; (3) presence of other malignancies; (4) coexistence of autoimmune diseases; (5) severe organic diseases; (6) uncontrolled systemic infections; and (7) inability to assess tumor regression.

All eligible patients were randomly assigned to the training set (70%) and the test set (30%) using simple randomization before model development and validation. This study was conducted in accordance with the Declaration of Helsinki and received approval from the Ethics Committee of Gansu Provincial Maternal and Child Health Hospital (Approved No. 2022GSFY48). Given the retrospective nature of the study, the requirement for informed consent was waived by the Ethics Committee. All patient data were anonymized and de-identified prior to analysis, and patient confidentiality was strictly protected throughout the study.

Concurrent Chemoradiotherapy

All patients underwent CCRT as the standard treatment for LACC. The concurrent chemotherapy was primarily cisplatin-based, with carboplatin used as an alternative in patients with impaired renal function. Two chemotherapy regimens were utilized based on patient tolerability, tumor stage, and interim response: (1) a three-weekly regimen consisting of paclitaxel liposome (135 mg/m²) or nab-paclitaxel (260 mg/m²) combined with cisplatin (75 mg/m²) administered intravenously on day 1 every 21 days, for a total of one to two cycles; and (2) a weekly regimen comprising paclitaxel liposome (75 mg/m²) or nab-paclitaxel (100 mg/m²) combined with cisplatin (40 mg/m²) given once weekly for two to six cycles. Chemotherapeutic agents were infused intravenously over at least 60 minutes, accompanied by adequate hydration. Dose adjustments were allowed in cases of grade ≥ 3 chemotherapy-related toxicities.

Radiotherapy Planning and Administration

Prior to radiotherapy, patients were instructed to empty their rectum and bladder, then drink 600 mL of water to maintain moderate bladder filling during treatment. Patients were immobilized in a supine position using individualized vacuum immobilization molds, with laser alignment ensuring reproducible patient positioning. Radiotherapy planning was conducted using high-resolution CT simulations (slice thickness 3 mm) to precisely delineate gross tumor volume, clinical target volume (CTV), and organs at risk. Target volume delineation was independently performed by two senior radiation oncologists, and consensus was reached through discussion to resolve discrepancies. External beam radiotherapy (EBRT) was delivered using volumetric modulated arc therapy (VMAT) via a Siemens PRIMUS linear accelerator. The pelvic planned target volume (PTV) received 45–51 Gy in 25–28 fractions (1.8–2 Gy per fraction), administered five times weekly. Patients presenting with para-aortic or pelvic lymph node metastases or primary tumors ≥ 4 cm received a simultaneous integrated boost to 60 Gy in 30 fractions.

Following EBRT, patients underwent high-dose-rate (HDR) intracavitary brachytherapy (ICBT) using an ¹⁹²Ir remote after loading system under CT guidance. ICBT delivered a total dose of 20–30 Gy in 4–6 fractions (5–6 Gy per fraction), once weekly, to the high-risk CTV at a reference depth of 0.5 cm (equivalent to Point A). Patients who were unsuitable for ICBT received an EBRT boost of 10 Gy delivered in 5 fractions. Dose constraints for organs at risk were applied according to the GEC-ESTRO guidelines, specifically limiting D_{2cc} of the bladder to ≤ 75 Gy_{EQD2} and rectum to ≤ 70 Gy_{EQD2}.

Treatment Response Assessment

Clinical efficacy was evaluated approximately 8 weeks (± 7 days) after completion of the last brachytherapy or EBRT boost fraction, based on version 1.1 of the Response Evaluation Criteria in Solid Tumors (RECIST 1.1).²⁴ Assessment modalities included pelvic examination and colposcopy by a gynecologic oncologist, contrast-enhanced pelvic MRI (T1/T2-weighted and diffusion-weighted imaging sequences) for detailed measurement of primary tumor and lymph node status, and contrast-enhanced CT of the chest and abdomen to exclude distant metastases. In cases of inconclusive CT or MRI findings, ¹⁸F-FDG PET/CT scans were performed. Tumor responses were categorized as complete response (CR; complete disappearance of lesions), partial response (PR; $\geq 30\%$ reduction), stable disease (SD; neither sufficient shrinkage nor increase), or progressive disease (PD; $\geq 20\%$ increase or emergence of new lesions). Patients achieving CR or PR were classified into the treatment-sensitive group, whereas those with SD or PD were assigned to the treatment-resistant group.

Body Composition Measurement

Prior to initial treatment, a single axial CT image at the level of the third lumbar vertebra (L3) was used to quantify skeletal muscle and adipose tissue. The L3 level was identified by a board-certified radiologist as the slice where both transverse processes were fully visualized. Two trained readers, blinded to clinical outcomes, performed segmentation in SliceOmatic (version 5.0; TomoVision, Magog, Canada) using semi-automated thresholding with manual correction. Skeletal muscle (psoas, paraspinal, transversus abdominis, rectus abdominis, and internal/external obliques) was segmented at -29 to $+150$ HU. Adipose tissue was segmented with standard HU ranges, with subcutaneous and intermuscular adipose at -190 to -30 HU and visceral adipose at -150 to -50 HU. Cross-sectional areas (cm^2) were normalized by height squared (m^2) to obtain the skeletal muscle index (SMI), visceral adipose index (VAI), subcutaneous adipose index (SAI), and intramuscular adipose index (IMAI), respectively. Inter-reader reproducibility for SMI, SAI, VAI, and IMAI was quantified using ICC (two-way random-effects, absolute-agreement), Bland-Altman analysis, and within-subject CV. Inter-reader agreement was excellent across all L3-derived metrics (all ICCs ≥ 0.96) with minimal bias and narrow 95% limits of agreement ([Supplementary Table S1](#)).

Systemic Inflammatory Biomarkers

Baseline laboratory parameters, including platelet count, neutrophil count, monocyte count, lymphocyte count, red blood cell distribution width (RDW), and serum albumin levels, were obtained from complete blood counts conducted within one week prior to treatment initiation. Derived inflammatory biomarkers were calculated as follows: neutrophil-to-lymphocyte ratio (NLR), neutrophil-to-platelet ratio (NPR), platelet-to-lymphocyte ratio (PLR), and lymphocyte-to-monocyte ratio (LMR). Additionally, the prognostic nutritional index (PNI) was calculated using the formula: serum albumin (g/L) $+ 5 \times$ lymphocyte count ($10^9/\text{L}$). The systemic immune-inflammation index (SII) was determined using the formula: neutrophil count \times platelet count / lymphocyte count ($10^9/\text{L}$).

Statistical Method

All statistical analyses were performed using SPSS version 27.0 (IBM, Armonk, NY, USA) and R version 4.4.2. The R packages utilized included “RMS”, “glmnet”, “caret”, and “foreign”. Categorical data were presented as frequencies and percentages, and comparisons between groups were conducted using the Chi-square test or Fisher’s exact test as appropriate. Continuous variables following a normal distribution were expressed as mean \pm standard deviation and compared using Student’s *t*-test. Continuous variables without normal distributions were reported as median (interquartile range) and compared using the Mann–Whitney *U*-test. Multivariate logistic regression analysis was employed to identify independent predictive factors for CCRT response. The Hosmer–Lemeshow test was utilized to assess the goodness-of-fit of the logistic regression model. Receiver operating characteristic (ROC) curves and the area under the curve (AUC) were generated to evaluate the overall accuracy and discriminative ability of the predictive model. The difference between AUCs was determined by the DeLong test. In addition, a calibration curve and clinical decision curve analysis (DCA) were used to evaluate the goodness of fit and clinical practicability of the nomogram. These analyses were performed to identify independent predictors of CCRT sensitivity and to evaluate the discrimination, calibration, and potential clinical utility of the nomogram. All statistical tests were two-sided, and a *p*-value of less than 0.05 was considered statistically significant.

Results

Patients

A total of 215 patients met the inclusion and exclusion criteria, including 150 patients in the sensitivity group and 65 in the resistance group. Using simple randomization, all eligible patients were assigned to the training set (70%, $n = 150$) and the test set (30%, $n = 65$) for model development and validation. Baseline clinicopathologic characteristics, systemic inflammatory markers, and body composition parameters were comparable between the training and test sets, with no statistically significant differences observed ([Table 1](#)), indicating that the two cohorts were well balanced.

Table 1 Baseline Characteristics of the Training and Test Sets

Variables	Training Set (n = 150)	Test Set (n = 65)	t/Z/ χ^2	P
Age	52.44 ± 12.39	51.38 ± 12.32	0.57	0.566
Tumor size	5.55 ± 1.41	5.33 ± 1.30	1.068	0.287
LMR	2.78 ± 1.18	2.74 ± 1.13	0.18	0.861
NLR	2.92 ± 1.20	2.82 ± 1.17	0.59	0.559
NPR	0.02 (0.01, 0.02)	0.01 (0.01, 0.02)	-1.34	0.181
PLR	174.86 (143.87, 224.62)	190.72 (154.74, 244.12)	-1.45	0.147
RDW	13.06 ± 1.72	13.49 ± 1.76	-1.67	0.096
PNI	41.63 ± 6.53	41.43 ± 6.33	0.21	0.831
SII	546.88 (421.01, 820.01)	640.59 (470.38, 883.75)	-1.58	0.115
BMI	25.42 ± 2.56	25.08 ± 2.43	0.89	0.373
SMI	45.92 ± 8.23	46.64 ± 8.06	-0.59	0.557
SAI	93.25 ± 14.56	92.81 ± 13.40	0.21	0.837
VAI	29.35 ± 5.45	29.45 ± 5.60	-0.11	0.910
IMAI	7.03 ± 1.65	6.98 ± 1.68	0.21	0.837
Response			0.58	0.448
Resistance	43 (28.67)	22 (33.85)		
Sensitivity	107 (71.33)	43 (66.15)		
Smoking			1.97	0.160
No	133 (88.67)	53 (81.54)		
Yes	17 (11.33)	12 (18.46)		
Stage (Figo 2018)			0.15	0.929
II	18 (12.00)	9 (13.85)		
III	123 (82.00)	52 (80.00)		
IV	9 (6.00)	4 (6.15)		
Squamous cell carcinoma			0.00	1.000
No	7 (4.67)	3 (4.62)		
Yes	143 (95.33)	62 (95.38)		
Tumor grade			0.44	0.803
G1	22 (10.23)	14 (9.33)		
G2	74 (34.42)	52 (34.67)		
G3	119 (55.35)	84 (56.00)		

Notes: FIGO stages II, III, and IV refer to the 2018 FIGO staging system. t, Student's *t*-test; Z, Mann-Whitney *U*-test; χ^2 , chi-square test.

Abbreviations: LMR, lymphocyte-to-monocyte ratio; NLR, neutrophil-to-lymphocyte ratio; NPR, neutrophil-to-platelet ratio; PLR, platelet-to-lymphocyte ratio; RDW, red blood cell distribution width; PNI, prognostic nutritional index; SII, systemic immune-inflammation index; BMI, body mass index; SMI, skeletal muscle index; SAI, subcutaneous adipose index; VAI, visceral adipose index; IMAI, intramuscular adipose index.

Screening of Clinical Characteristics

Within the training set, 107 patients were classified as CCRT-sensitive and 43 as CCRT-resistant. Compared with the resistant group, the sensitive group showed significantly smaller tumor size and lower PLR, RDW, SII, and VAI, but higher PNI and SMI (all $P < 0.05$; Table 2). These findings suggest that both host inflammatory/nutritional status and body composition may be associated with sensitivity to CCRT in patients with LACC.

Establishment of the Nomogram

Variables that were significant in the univariate analysis were entered into a multivariable logistic regression model to identify independent predictors of CCRT sensitivity in patients with LACC. Tumor size (OR = 0.657, 95% CI: 0.474–0.912, $P = 0.012$), PLR (OR = 0.992, 95% CI: 0.985–1.000, $P = 0.049$), PNI (OR = 1.133, 95% CI: 1.055–1.217, $P = 0.001$), SMI (OR = 1.079, 95% CI: 1.021–1.141, $P = 0.007$), and VAI (OR = 0.913, 95% CI: 0.844–0.987, $P = 0.023$) were identified as independent predictors (Table 3). These variables, representing both tumor-related and host-related characteristics, were incorporated into the final nomogram (Figure 1), which provides an

Table 2 Comparison of Clinicopathologic Characteristics, Inflammatory Biomarkers, and Body Composition Metrics Between CCRT Sensitivity and Resistance Groups in the Training Set

Variables	Resistant Group (n = 43)	Sensitive Group (n = 107)	t/Z/ χ^2	P
Age	54.44 ± 11.07	51.64 ± 12.85	1.26	0.211
Tumor size	5.92 ± 1.44	5.40 ± 1.38	2.03	0.044
LMR	3.04 ± 1.13	2.67 ± 1.19	1.72	0.087
NLR	2.99 ± 1.38	2.89 ± 1.13	0.44	0.659
NPR	0.01 (0.01, 0.02)	0.02 (0.01, 0.02)	-1.34	0.179
PLR	195.36 (173.62, 232.61)	165.78 (137.20, 208.66)	-3.18	0.001
RDW	13.52 ± 1.64	12.88 ± 1.73	2.08	0.039
PNI	39.35 ± 5.64	42.55 ± 6.66	-2.78	0.006
SII	662.12 (482.31, 964.33)	513.30 (403.46, 680.47)	-2.81	0.005
BMI	25.31 ± 2.22	25.46 ± 2.70	-0.31	0.757
SMI	43.30 ± 8.44	46.98 ± 7.94	-2.52	0.013
SAI	93.67 ± 14.23	93.08 ± 14.75	0.22	0.822
VAI	31.11 ± 5.63	28.65 ± 5.24	2.54	0.012
IMAI	6.91 ± 1.49	7.08 ± 1.72	-0.56	0.574
Smoking			0.13	0.721
No	37 (86.05)	96 (89.72)		
Yes	6 (13.95)	11 (10.28)		
Stage (Figo 2018)			0.35	0.839
II	6 (13.95)	12 (11.21)		
III	34 (79.07)	89 (83.18)		
IV	3 (6.98)	6 (5.61)		
Squamous cell carcinoma			1.66	0.197
No	0 (0.00)	7 (6.54)		
Yes	43 (100.00)	100 (93.46)		
Tumor grade			0.41	0.815
G1	14 (9.33)	3 (6.98)		
G2	52 (34.67)	15 (34.88)		
G3	84 (56.00)	25 (58.14)		

Notes: FIGO stages II, III, and IV refer to the 2018 FIGO staging system. t, Student's t-test; Z, Mann-Whitney U-test; χ^2 , chi-square test. Bold values indicate statistical significance ($P < 0.05$).

Abbreviations: LMR, lymphocyte-to-monocyte ratio; NLR, neutrophil-to-lymphocyte ratio; NPR, neutrophil-to-platelet ratio; PLR, platelet-to-lymphocyte ratio; RDW, red blood cell distribution width; PNI, prognostic nutritional index; SII, systemic immune-inflammation index; BMI, body mass index; SMI, skeletal muscle index; SAI, subcutaneous adipose index; VAI, visceral adipose index; IMAI, intramuscular adipose index.

Table 3 Multivariate Logistic Regression Analysis Identifying Independent Predictors of CCRT Sensitivity in the Training Set

	B	Se	Wald	P	OR	95% CI of OR	
Tumor size (cm)	-0.42	0.167	6.298	0.012	0.657	0.474	0.912
PLR	-0.008	0.004	3.874	0.049	0.992	0.985	1
RDW	-0.134	0.131	1.056	0.304	0.874	0.676	1.13
PNI	0.125	0.036	11.691	0.001	1.133	1.055	1.217
SII	-0.001	0.001	1.071	0.301	0.999	0.998	1.001
SMI	0.076	0.028	7.202	0.007	1.079	1.021	1.141
VAI	-0.091	0.04	5.179	0.023	0.913	0.844	0.987
Intercept	1.338	2.848	0.221	0.639	3.81		

Note: Bold values indicate statistical significance ($P < 0.05$).

Abbreviations: B, regression coefficient; SE, standard error; OR, odds ratio; CI, confidence interval.

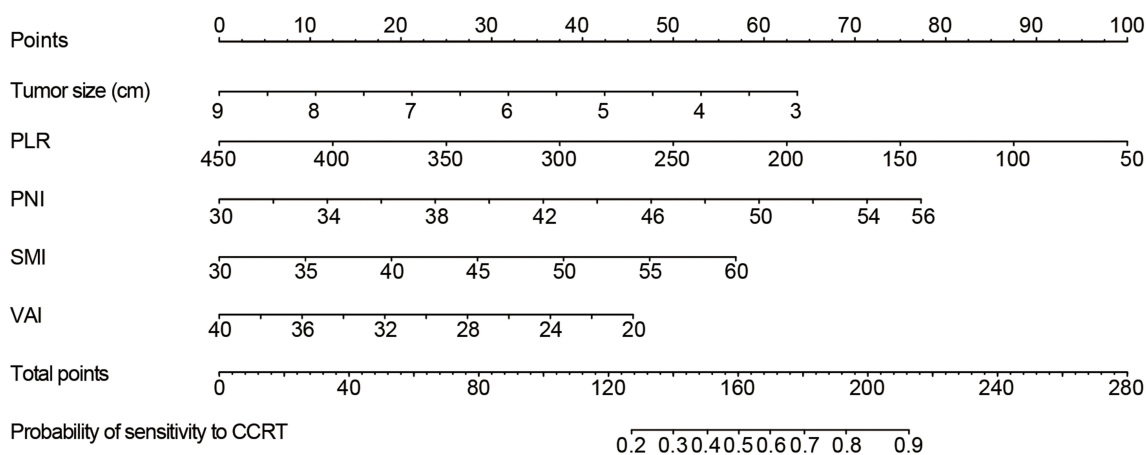


Figure 1 Nomogram for predicting concurrent chemoradiotherapy sensitivity in locally advanced cervical cancer. A nomogram was developed for predicting the sensitivity to CCRT in patients with LACC. The nomogram integrates five key predictors: tumor size, PLR, PNI, SMI, and VAI. Each predictor is assigned a specific score along the “Points” axis based on its value. The total score is calculated by summing the individual scores, which corresponds to the probability of sensitivity to CCRT shown on the bottom scale.

individualized probability of CCRT sensitivity based on the combined effect of these predictors. The training set included 107 sensitive events, corresponding to an events-per-variable ratio of 21.4. Bootstrap internal validation with 1000 resamples showed that the same five predictors remained significant, with coefficient estimates similar to those of the original model ([Supplementary Table S2](#)), indicating good model stability.

Test of the Nomogram

The nomogram showed good calibration and discrimination in both the training and test sets. The Hosmer-Lemeshow test indicated an adequate model fit ($\chi^2 = 8.679$, $P = 0.370$). Calibration curves demonstrated good agreement between predicted and observed probabilities of CCRT sensitivity in the training set ([Figure 2A](#)) and test set ([Figure 2B](#)), with mean absolute errors of 0.037 and 0.020, respectively. In ROC analysis, the nomogram achieved an AUC of 0.796 (95% CI: 0.714–0.878) in the training set and 0.751 (95% CI: 0.618–0.884) in the test set ([Figure 3A](#) and [B](#)). Using the optimal cutoff value of 0.66, the sensitivity and specificity were 75.7% and 72.1% in the training set, and 79.1% and 59.1% in the test set, respectively. Overall, these results indicate that the nomogram had good discriminatory ability and satisfactory predictive performance.

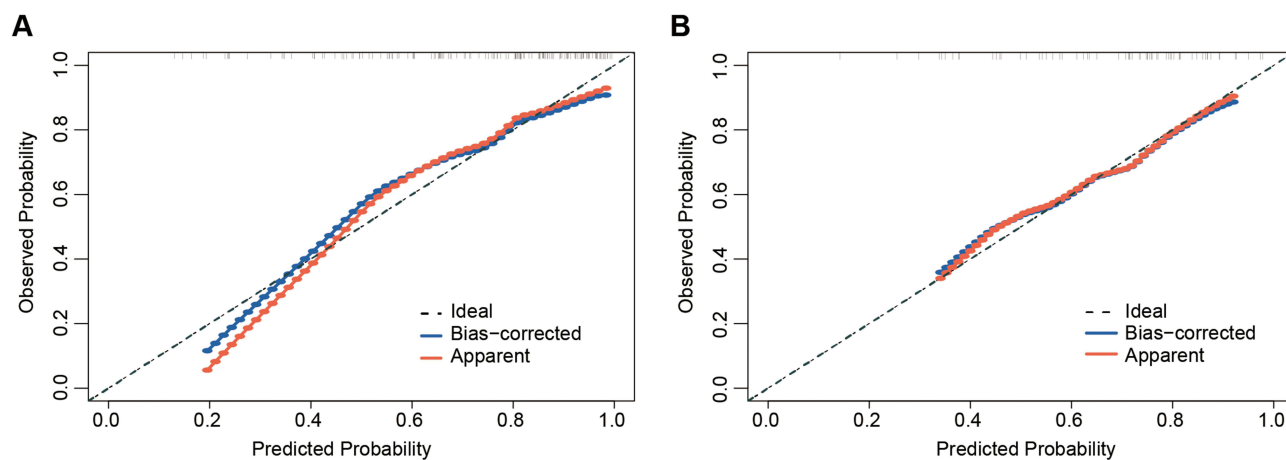


Figure 2 Calibration curves for the nomogram. (**A-B**) Calibration curves for the nomogram in the (**A**) training set and (**B**) test sets. The X-axis represents the predicted probability of CCRT sensitivity based on the nomogram, while the Y-axis represents the actual probability of CCRT sensitivity occurrence. The diagonal line represents the ideal prediction scenario. The red line indicates the calibration curve for the overall sample, and the blue line represents the calibration curve derived from boot-strapping with 1,000 resamples ($B = 1000$).

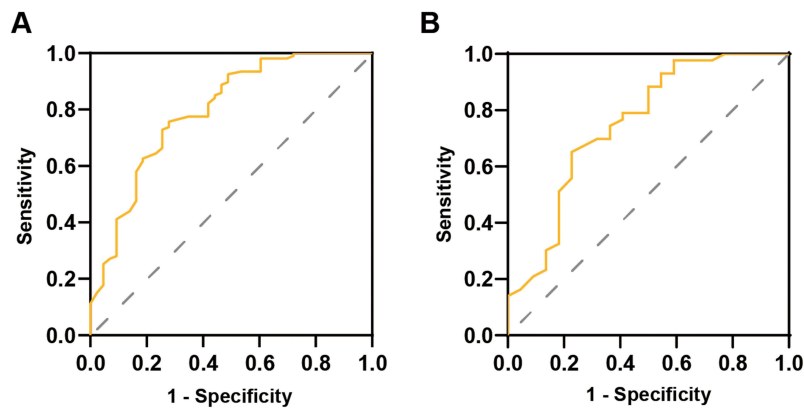


Figure 3 Receiver operating characteristic (ROC) curves for the nomogram in the training and test sets. **(A)** In the training set, the ROC curves demonstrated high predictive accuracy of nomogram with an AUC of 0.796 (95% CI: 0.723–0.858). The optimal cutoff value was 0.66, corresponding to a sensitivity of 75.7% and a specificity of 72.09%. **(B)** In the test set, the nomogram achieved an AUC of 0.751 (95% CI: 0.618–0.884). With a cutoff value of 0.66, the model demonstrated a sensitivity of 79.07% and a specificity of 59.09%. The Orange solid line indicates the ROC curve of the nomogram, and the gray diagonal dashed line indicates the line of no discrimination.

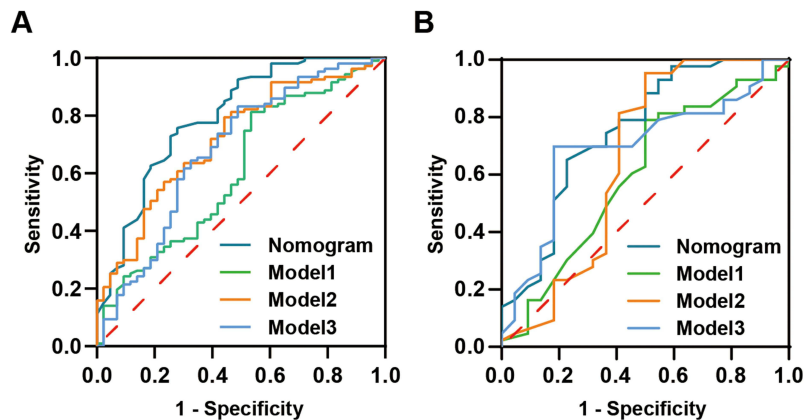


Figure 4 Comparative analysis of predictive performance between the nomogram and single-domain models. **(A)** Training set. **(B)** Test set. Receiver operating characteristic (ROC) curves comparing the nomogram, the clinical model (Model 1, including tumor size), the systemic inflammatory model (Model 2, incorporating PLR and PNI), and the body composition model (Model 3, comprising SMI and VAI). The dark cyan, green, Orange, and light blue solid lines represent the ROC curves of the nomogram, Model 1, Model 2, and Model 3, respectively. The red diagonal dashed line represents the reference line indicating no discrimination.

Comparison of Predictive Accuracy and Clinical Applicability of the Nomogram

To further assess the added value of the integrated model, we compared the nomogram with three single-domain models: a clinical model (Model 1, tumor size only), a systemic inflammatory model (Model 2, PLR and PNI), and a body composition model (Model 3, SMI and VAI). The nomogram consistently showed better discriminatory performance than the three single-domain models in both the training and test sets (Figure 4 and Supplementary Table S3), indicating the advantage of integrating multidimensional predictors. Decision curve analysis further demonstrated that the nomogram provided a higher net benefit across a range of threshold probabilities in both cohorts (Figure 5), supporting its potential clinical utility. These findings support the advantage of integrating tumor-related, inflammatory, and body composition variables into a multidimensional predictive model.

Discussion

In this study, we developed and validated a novel nomogram combining body composition metrics and systemic inflammatory markers to predict CCRT response in LACC. The nomogram is based on tumor size, PLR, PNI, SMI, and VAI. It demonstrated good discrimination in both the training and test cohorts, together with favorable calibration and clinical utility, supporting its potential value as a predictive tool. This model provides a non-invasive, clinically

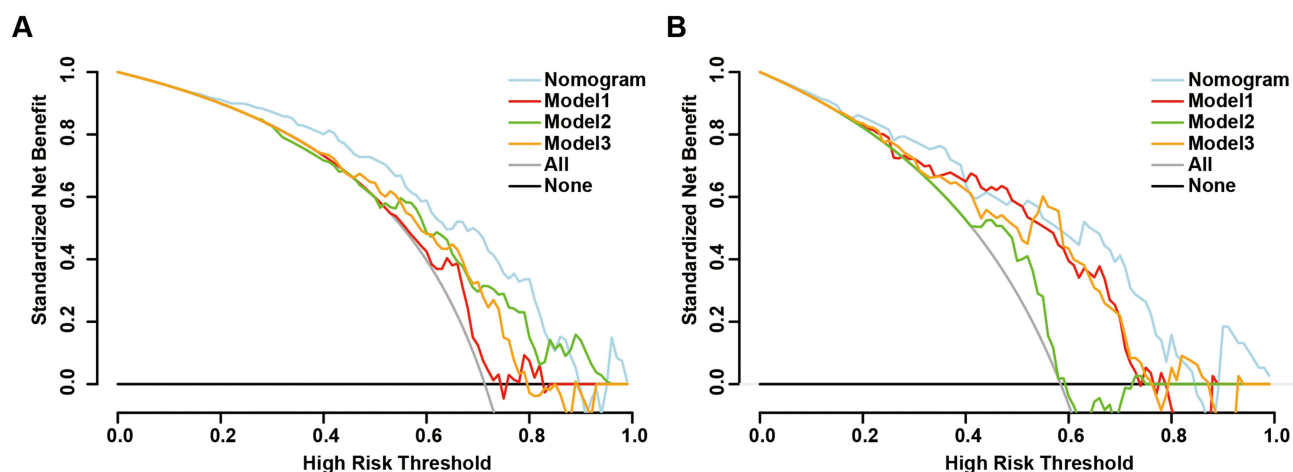


Figure 5 Decision curve analysis (DCA) of the nomogram and three single-domain models. (A–B) DCA was performed to compare the net clinical benefit of the nomogram, the clinical model (Model 1, including tumor size), the systemic inflammatory model (Model 2, incorporating PLR and PNI), and the body composition model (Model 3, comprising SMI and VAI) across a range of high-risk threshold probabilities in the (A) training set and (B) test sets. The light blue, red, green, and Orange curves represent the nomogram, Model 1, Model 2, and Model 3, respectively. The gray line (“All”) indicates the strategy of considering all patients as high risk, and the black line (“None”) indicates the strategy of considering no patients as high risk. Higher standardized net benefit indicates greater clinical utility at the corresponding high-risk threshold.

feasible tool to identify patients most likely to benefit from CCRT, facilitating personalized treatment planning, optimizing resource allocation, and ultimately improving patient outcomes in the management of LACC.

Systemic inflammatory markers have gained prominence as vital prognostic indicators in various malignancies, reflecting the intricate interplay between the immune system and tumor biology.^{22,25} Among the systemic inflammatory and nutritional variables, PLR and PNI were independently associated with CCRT sensitivity in our cohort. This finding is generally consistent with previous studies. In particular, Gangopadhyay et al analyzed 583 women with LACC and showed that baseline PNI was significantly associated with complete clinical response after chemoradiation, with an optimal cutoff value of 44.8 and an AUC of 0.813.²⁶ More recently, He et al, in a two-center retrospective cohort of 622 patients with LACC receiving CCRT, also identified inflammatory markers including PLR as independent predictors of short-term therapeutic response.²³ Taken together, these data support the view that pretreatment immunonutritional status is closely related to radiosensitivity and chemosensitivity in cervical cancer. The underlying mechanisms may involve the modulation of the tumor microenvironment by inflammatory cells, where an elevated PLR signifies a predominance of lymphocyte and platelets that facilitate tumor progression and therapeutic resistance, while a higher PNI indicates robust immune function capable of enhancing therapeutic responses.^{27–29} Our findings reinforce the prognostic value of systemic inflammatory markers, highlighting their potential utility in clinical decision-making for LACC management.

Beyond traditional prognostic factors, body composition metrics derived from CT scans provide a more nuanced assessment of a patient’s physiological state, surpassing the limitations of BMI in capturing muscle and adipose tissue distribution.³⁰ We also found that body composition parameters, particularly higher SMI and lower VAI, were independently associated with favorable early response. This observation is biologically plausible and extends the clinical relevance of host-related body composition markers in cervical cancer. Guo et al reported in 196 patients with LACC treated with CCRT that high SII, sarcopenia (low SMI), high SAI, and high VAI were independent risk factors for overall survival, and further developed a nomogram combining body composition and systemic inflammatory markers.²² Compared with that survival-oriented model, our study suggests that CT-derived body composition may also be informative at an earlier stage of treatment evaluation. In other words, the contribution of body composition in LACC may extend beyond long-term prognosis to the prediction of short-term response. A possible explanation is that preserved skeletal muscle reflects better metabolic and immune reserve, whereas excess visceral adiposity may promote a chronic inflammatory milieu that is less favorable for treatment response.³¹

Our findings should also be interpreted in the broader context of predictive modeling for cervical cancer treated with CCRT. Existing models have mainly focused on long-term endpoints such as progression-free survival or overall

survival, or have relied primarily on clinicopathological and laboratory variables. For example, Hua et al developed a survival nomogram for patients with LACC undergoing CCRT with or without adjuvant chemotherapy, while Wang et al constructed ALI-based nomograms for PFS and OS in cervical squamous cell carcinoma receiving CCRT.^{32,33} More recently, He et al developed dual nomogram models for both short-term therapeutic response and overall survival. In that study, tumor stage, histological differentiation, depth of stromal invasion, NLR, and PLR were identified as independent predictors of treatment response, whereas the OS nomogram showed good performance across the training, internal validation, and external validation cohorts.²³ These studies collectively support the value of integrated prediction models in this setting; however, they remain largely centered on clinicopathological and laboratory indicators. By contrast, our model incorporates routinely available pretreatment blood biomarkers together with CT-based body composition parameters and directly shows that this multidimensional framework performs better than single-domain approaches for early CCRT sensitivity prediction. From a theoretical perspective, this supports a more comprehensive framework in which treatment response is jointly determined by tumor burden and host inflammatory, nutritional, and metabolic reserve. From a practical perspective, all variables included in the nomogram are non-invasive and routinely obtainable during standard pretreatment assessment, which may facilitate early risk stratification and individualized management in real-world settings. However, the model should be regarded as an early risk-stratification tool rather than a substitute for guideline-based treatment indications.

Several limitations should be acknowledged. First, this was a retrospective single-center study, which may introduce selection bias and limit generalizability. Second, the primary endpoint was early radiologic response assessed at approximately 8 weeks after treatment, which should be interpreted as a short-term outcome rather than a validated surrogate for progression-free or overall survival. Third, external validation was not available, and dynamic changes in body composition and inflammatory markers during treatment were not assessed. Finally, additional biomarkers, including molecular features, may further improve predictive performance. Therefore, future multicenter prospective studies are needed to externally validate the model, clarify its association with long-term survival outcomes, and explore whether integrating molecular or longitudinal markers can further enhance predictive accuracy.

Conclusions

In conclusion, we developed and internally validated a nomogram integrating tumor size, systemic inflammatory markers, and CT-based body composition parameters for early prediction of CCRT sensitivity in LACC. Our findings indicate that combining tumor- and host-related factors provides a more comprehensive predictive approach than single-domain models. This supports the concept that treatment response is influenced by both tumor burden and host inflammatory, nutritional, and body composition status. Given that all variables are routinely available, the model may facilitate early risk stratification and individualized treatment planning. However, due to the retrospective single-center design and the exploratory nature of early-response prediction, further external validation and incorporation of additional biomarkers are required.

AI Declarations

AI-assisted tools were used solely for language refinement and drafting support. No AI tools were used for data generation, statistical analysis, or image generation.

Data Sharing Statement

The datasets used and/or analyzed during the current study are available from the corresponding author on reasonable request.

Ethics Approval

This study was conducted in accordance with the Declaration of Helsinki and received approval from the Ethics Committee of Gansu Provincial Maternal and Child Health Hospital (Approved No. 2022GSFY48). Given the retrospective nature of the study, the requirement for informed consent was waived by the Ethics Committee. All patient data

were anonymized and de-identified prior to analysis, and patient confidentiality was strictly protected throughout the study.

Author Contributions

All authors made a significant contribution to the work reported, whether that is in the conception, study design, execution, acquisition of data, analysis and interpretation, or in all these areas; took part in drafting, revising or critically reviewing the article; gave final approval of the version to be published; have agreed on the journal to which the article has been submitted; and agree to be accountable for all aspects of the work.

Funding

This work was supported by the Gansu Provincial Health Industry Research Project (Grant No. GSWSHL2023-10), the Natural Science Foundation of Gansu Province (Grant No. 2022JR5RA724, 22JR5RA722).

Disclosure

The authors declare that they have no competing interests.

References

1. Cibula D, Raspollini MR, Planchamp F, et al. ESGO/ESTRO/ESP Guidelines for the management of patients with cervical cancer - update 2023. *Virchows Arch.* 2023;482(6):935–966. doi:10.1007/s00428-023-03552-3
2. Bray F, Laversanne M, Sung H, et al. Global cancer statistics 2022: GLOBOCAN estimates of incidence and mortality worldwide for 36 cancers in 185 countries. *CA Cancer J Clin.* 2024;74(3):229–263. doi:10.3322/caac.21834
3. Tewari KS. Cervical Cancer. *N Engl J Med.* 2025;392(1):56–71. doi:10.1056/NEJMra2404457
4. Koh W-J, Abu-Rustum NR, Bean S, et al. Cervical cancer, version 3.2019, NCCN clinical practice guidelines in oncology. *J Natl Compr Canc Netw.* 2019;17(1):64–84. doi:10.6004/jnccn.2019.0001
5. Francoeur AA, Monk BJ, Tewari KS. Treatment advances across the cervical cancer spectrum. *Nat Rev Clin Oncol.* 2025;22(3):182–199. doi:10.1038/s41571-024-00977-w
6. Cohen PA, Jhingran A, Oaknin A, et al. Cervical cancer. *Lancet.* 2019;393(10167):169–182. doi:10.1016/S0140-6736(18)32470-X
7. Morris M, Eifel PJ, Lu J, et al. Pelvic radiation with concurrent chemotherapy compared with pelvic and para-aortic radiation for high-risk cervical cancer. *N Engl J Med.* 1999;340(15):1137–1143. doi:10.1056/NEJM199904153401501
8. Uke A, Dahake SB, Luharia A, et al. Investigating and analyzing prognostic factors and their impact on recurrent cervical cancers. *Cureus.* 2024;16(7):e65361. doi:10.7759/cureus.65361
9. Eifel PJ, Winter K, Morris M, et al. Pelvic irradiation with concurrent chemotherapy versus pelvic and para-aortic irradiation for high-risk cervical cancer: an update of radiation therapy oncology group trial (RTOG) 90-01. *J Clin Oncol.* 2004;22(5):872–880. doi:10.1200/JCO.2004.07.197
10. Yao G, Qiu J, Zhu F, et al. Survival of patients with cervical cancer treated with definitive radiotherapy or concurrent chemoradiotherapy according to histological subtype: a systematic review and meta-analysis. *Front Med Lausanne.* 2022;9:843262. doi:10.3389/fmed.2022.843262
11. Gao S, Du S, Lu Z, et al. Multiparametric PET/MR (PET and MR-IVIM) for the evaluation of early treatment response and prediction of tumor recurrence in patients with locally advanced cervical cancer. *Eur Radiol.* 2020;30(2):1191–1201. doi:10.1007/s00330-019-06428-w
12. Abrar SS, Azmel Mohd Isa S, Mohd Hairon S, et al. Prognostic factors for cervical cancer in Asian populations: a scoping review of research from 2013 to 2023. *Cureus.* 2024;16(10):e71359. doi:10.7759/cureus.71359
13. Venkat PS, Smick AH, Salani R. Current opinions: updates on the changing landscape in the management of cervical cancer. *Curr Opin Obstet Gynecol.* 2025;37(1):16–21. doi:10.1097/GCO.0000000000000999
14. Buttarelli M, Babini G, Raspaglio G, et al. A combined ANXA2-NDRG1-STAT1 gene signature predicts response to chemoradiotherapy in cervical cancer. *J Exp Clin Cancer Res.* 2019;38(1):279. doi:10.1186/s13046-019-1268-y
15. Miranda AVSSD, Da Silva JL, Andrade DAPD, et al. Stereotactic body radiotherapy boost as an alternative to brachytherapy for cervical cancer: a scoping review. *Crit Rev Oncol Hematol.* 2024;204:104517. doi:10.1016/j.critrevonc.2024.104517
16. Tian M, Xu H, Wang H, et al. Pretreatment computed tomography-defined sarcopenia, treatment-associated muscle loss, and survival in patients with cervical cancer: a systematic review and meta-analysis. *Nutr Rev.* 2024;83.
17. Xie H, Ruan G, Ge Y, et al. Inflammatory burden as a prognostic biomarker for cancer. *Clin Nutr.* 2022;41(6):1236–1243. doi:10.1016/j.clnu.2022.04.019
18. Yamamoto T, Kawada K, Obama K. Inflammation-Related biomarkers for the prediction of prognosis in colorectal cancer patients. *Int J Mol Sci.* 2021;22(15):8002. doi:10.3390/ijms22158002
19. Meng L, Yang Y, Hu X, et al. Prognostic value of the pretreatment systemic immune-inflammation index in patients with prostate cancer: a systematic review and meta-analysis. *J Transl Med.* 2023;21(1):79. doi:10.1186/s12967-023-03924-y
20. Dinca A-L, Diaconu A, Birla RD, et al. Systemic inflammation factors as survival prognosis markers in ovarian neoplasm and the relationship with cancer-associated inflammatory mediators-a review. *Int J Immunopathol Pharmacol.* 2023;37:3946320231178769. doi:10.1177/03946320231178769
21. López-Hernández D. Epidemiological association between body fat percentage and cervical cancer: a cross-sectional population-based survey from Mexico. *Arch Med Res.* 2013;44(6):454–458. doi:10.1016/j.arcmed.2013.08.007

22. Guo H, Feng S, Li Z, et al. Prognostic value of body composition and systemic inflammatory markers in patients with locally advanced cervical cancer following chemoradiotherapy. *J Inflamm Res.* 2023;16:5145–5156. doi:10.2147/JIR.S435366
23. He Z, Lai J, Lin W, et al. Prognostic value of the lactate dehydrogenase-to-albumin ratio (LAR) combined with clinicopathological indicators for predicting outcomes in locally advanced cervical cancer undergoing concurrent chemoradiotherapy: a retrospective cohort study and nomogram development. *Am J Cancer Res.* 2026;16(2):470–495. doi:10.62347/EHDB3254
24. Therasse P, Arbuck SG, Eisenhauer EA, et al. New guidelines to evaluate the response to treatment in solid tumors. European Organization for Research and Treatment of Cancer, National Cancer Institute of the United States, National Cancer Institute of Canada. *J Natl Cancer Inst.* 2000;92(3):205–216. doi:10.1093/jnci/92.3.205
25. Di Meglio A, Havas J, Pagliuca M, et al. A bio-behavioral model of systemic inflammation at breast cancer diagnosis and fatigue of clinical importance 2 years later. *Ann Oncol.* 2024;35(11):1048–1060. doi:10.1016/j.annonc.2024.07.728
26. Gangopadhyay A. Prognostic nutritional index and clinical response in locally advanced cervical cancer. *Nutr Cancer.* 2020;72(8):1438–1442. doi:10.1080/01635581.2020.1729820
27. Salati M, Filippi R, Vivaldi C, et al. The prognostic nutritional index predicts survival and response to first-line chemotherapy in advanced biliary cancer. *Liver Int.* 2020;40(3):704–711. doi:10.1111/liv.14314
28. Li S, Lu Z, Wu S, et al. The dynamic role of platelets in cancer progression and their therapeutic implications. *Nat Rev Cancer.* 2024;24(1):72–87. doi:10.1038/s41568-023-00639-6
29. Hedrick CC, Malanchi I. Neutrophils in cancer: heterogeneous and multifaceted. *Nat Rev Immunol.* 2022;22(3):173–187. doi:10.1038/s41577-021-00571-6
30. Kim JE, O'connor LE, Sands LP, et al. Effects of dietary protein intake on body composition changes after weight loss in older adults: a systematic review and meta-analysis. *Nutr Rev.* 2016;74(3):210–224. doi:10.1093/nutrit/nuv065
31. Gómez-Banoy N, Ortiz EJ, Jiang CS, et al. Body mass index and adiposity influence responses to immune checkpoint inhibition in endometrial cancer. *J Clin Invest.* 2024;134(17). doi:10.1172/JCI180516
32. Hua L, Wei M, Feng C, et al. Nomogram for predicting survival in locally advanced cervical cancer with concurrent chemoradiotherapy plus or not adjuvant chemotherapy: a retrospective analysis based on 2018 FIGO staging. *Cancer Biother Radiopharm.* 2024;39(9):690–705. doi:10.1089/cbr.2023.0199
33. Wang XC, Xu XL, Wang SY, et al. Nomogram based on the advanced lung cancer inflammation index and other relevant clinical factors for patients with cervical squamous cell carcinoma undergoing concurrent chemoradiotherapy. *BMC Cancer.* 2025;25(1):1043. doi:10.1186/s12885-025-14465-6

Cancer Management and Research

Publish your work in this journal

Cancer Management and Research is an international, peer-reviewed open access journal focusing on cancer research and the optimal use of preventative and integrated treatment interventions to achieve improved outcomes, enhanced survival and quality of life for the cancer patient. The manuscript management system is completely online and includes a very quick and fair peer-review system, which is all easy to use. Visit <http://www.dovepress.com/testimonials.php> to read real quotes from published authors.

Submit your manuscript here: <https://www.dovepress.com/cancer-management-and-research-journal>

Dovepress
Taylor & Francis Group